C. R. Chimie 5 (2002) 845–854

S1631074802014571/REV

Rare-earth-doped transparent glass ceramics

M. Clara Gonçalves, Luís F. Santos, Rui M. Almeida*

Departamento de Engenharia de Materiais / ICEMS, Instituto Superior Técnico, av. Rovisco Pais, 1049-001 Lisboa, Portugal

Received 15 April 2002; accepted 16 October 2002

Abstract – Glass ceramics are a known class of polycrystalline ceramic materials, where, depending on the glass matrix and the particular crystalline phases, one can obtain materials with improved mechanical, thermal, electrical or optical properties. The characteristics and applications of optical glass ceramics are reviewed, with particular emphasis on rare-earth-doped transparent glass ceramics for photonics, including the search for new transparent glass ceramic compositions and the development of suitable methods to process such materials into functional devices. ***To cite this article: M. Clara Gonçalves et al., C. R. Chimie 5 (2002) 845–854*** © 2002 Académie des sciences / Éditions scientifiques et médicales Elsevier SAS

rare earth / glass ceramics / photonics

Résumé – Les vitrocéramiques constituent une classe bien connue de matériaux céramiques polycristallins qui, selon la matrice vitreuse et les phases cristallines, possèdent des propriétés mécaniques, thermiques, électriques ou optiques améliorées. Les caractéristiques et les applications optiques des vitrocéramiques sont passées en revue, avec une insistance particulière sur les vitrocéramiques transparentes et dopées en terres rares pour application photonique, incluant les recherches effectuées sur les compositions de nouvelles vitrocéramiques transparentes et le développement des méthodes appropriées pour inclure de tels matériaux dans des dispositifs possédant une fonction particulière. ***Pour citer cet article : M. Clara Gonçalves et al., C. R. Chimie 5 (2002) 845–854*** © 2002 Académie des sciences / Éditions scientifiques et médicales Elsevier SAS

terres rares / vitrocéramiques / photonique

1. Glass ceramics – historical view

Glass ceramics, discovered by S.D. Stookey (Corning Glass Works, USA) in the mid-1950s [1–4], are polycrystalline ceramic materials, formed through the controlled nucleation and crystallisation of glass, where the amount of residual glassy phase is usually less than 50%. The precursor glass is melted, quenched and shape-processed and is then thermally converted into a composite material formed by a crystalline phase dispersed within a glass matrix. The basis of controlled internal crystallisation lies in efficient nucleation, often enabled by a small amount of a nucleating agent, that allows the development of fine, randomly oriented grains, in a ceramic generally without voids, microcracks, or other porosity [5].

The development of practically useful glass ceramics is relatively recent, but the first attempts in this direction may be referenced to Réaumur [6], as long ago as 1739, who produced polycrystalline materials from soda–lime–silica glass; yet the control of the crystallisation process was not achieved. Further, the crystallisation was initiated at the surface, resulting in weak and brittle articles. Only some 200 years after Réaumur's work, a directed research program started at Corning Glass Works, leading to the discovery of photosensitive glasses [1–4] and to the first glass ceramics patents, PYROFLAM® [7] and VISIONS® [8]. These contain small amounts of copper, silver or gold, which can be precipitated in the form of very small crystals during heat treatment of the precursor glasses. Stookey [1–4] successfully made use of colloidal particles precipitated within the glass, as nucle-

* *Correspondence and reprints.*
E-mail address: rui.almeida@ist.utl.pt (R.M. Almeida).

ation sites for its controlled crystallisation. Stookey developed a wide range of glass compositions that contained titanium dioxide as the nucleating agent, which promoted phase separation. Since then, many different types of nucleating agents for glass-ceramic production have been reported [5].

From the early times of glass fabrication, the emphasis has been on preventing devitrification from occurring. Devitrification implies the growth of crystalline material and, if this occurs during the later stages of melting or during the shaping of glass, it has a very harmful effect. Therefore, many studies of devitrification have been carried out, in order to develop an understanding of the phenomenon and to enable it to be suppressed or controlled. Although some glass compositions are self-nucleating and volume nucleation occurs, crystallisation or devitrification in vitreous systems occurs most readily from the surface, where crystals are nucleated by flaws or other defect sites. Two kinetic processes are well known to precede devitrification: phase separation by nucleation and growth, the latter is generally or by spinodal decomposition. So far, only nucleation–growth has been shown to lead to optically transparent glass-ceramic material. Spinodal decomposition is generally viewed as a negative effect, since there is loss of glass transparency [9].

Depending on the glass host and the crystal phase compositions, one can obtain materials with improved mechanical, thermal, electrical or optical properties. The applications of glass ceramics have covered six major categories up to now – cook-top panels, dinnerware, electronics, medicine and dentistry, tough glass ceramics and optical materials. Low thermal expansion cook-top panels, woodstove windows and fire doors, represent today the commercially most attractive glass-ceramic product. In electronics, glass ceramics have found major application in microelectronic packaging and products like Fotoform® [10], Fotoceram® [10] and Foturan® [11] have been registered. In dentistry and medicine, where bioglass ceramics found wide use as implants for dental and bone prostheses, a series of new products have been developed and patented under the trademarks Bioglass® [12], Fluoride Bioglass® [13], Ceravital® [14], and Cerabone® [15]. Natural bones and teeth are multiphase materials with specific properties very difficult to simulate, where glass devitrification appears to be a very effective way to achieve improved properties, including machinability. Tough glass ceramics have been developed since the first well-known Macor® product [16], in which the easily cleaved crystalline mica decreased the sensitivity to flaw propagation to such an extent that it could be machined with normal metallic tools. At Corning Glass Works, a variety called Dicor® [17] was developed for use in dental restoration and, at the Otto Schott Institute in Jena [18], similar products have been developed. Special optical materials, where the dimensional stability, luminescence, or photosensitivity characteristics of glass ceramics can be exploited in a variety of new applications, including photorefractivity, non-linear optical behaviour or optical amplification, have also been fabricated. The best-known commercial optical glass-ceramic is Zerodur®, produced by Schott [19], first designed for large telescope mirror blanks, but now routinely used for laser gyroscopes in airplanes. The key property requirement in all these glass-ceramic applications is an extremely low coefficient of thermal expansion in the temperature interval of work.

The state-of-the-art in a new class of transparent glass-ceramic (TGC) materials will be discussed in the present paper, in connection with photonics. Two main aspects are related to the development of a new optical technology, the first being the search of novel material properties and the second, of equal importance, being the development of suitable methods to process these materials into functional devices. Both aspects are reviewed in the sections below, with emphasis on the first one.

2. Transparent glass ceramics

TGC can be obtained under several conditions, where the achievement of low optical absorption and scattering is essential. According to the Rayleigh–Gans theory, crystal sizes well bellow the wavelength of the incident light present negligible attenuation due to scattering, which, for visible light, represents particle radii lower than ~15 nm [20]. A refractive index difference between the amorphous and crystalline phases of less than 0.1 is also required [20]. However, according to Beall and Pinckney [20], based on Hopper's model [21], crystal sizes of 30 nm and differences in refractive index of 0.3 may be acceptable, provided the crystal spacing is not more than six times the average crystal size. TGC can also be obtained for even larger crystal sizes, if optical isotropy is achieved within the glass ceramic. In fact, β-quartz crystals up to 10 μm, in the SiO_2–Al_2O_3–MgO–ZnO–ZrO_2 system, still provide good transparency in the glass ceramic [20].

Some of the most promising applications of TGC are: large telescope mirror blanks, liquid crystal displays, solar cells and photonic devices. Precision optical equipment, such as telescope mirrors, requires extremely low expansion coefficient and high transmission. Glass ceramics such as Zerodur® – an aluminosilicate glass with 50-nm β-quartz crystals and with 70% of crystalline phase – has almost zero thermal

expansion ($0 \pm 0.02 \times 10^{-6}\ K^{-1}$) in the temperature range of 0–100 °C and ~ 90% transmittance between 0.6 and 2.0 μm [5, 9].

Liquid crystal displays for laptop computers are based on TGC of lithium aluminosilicate compositions, with β-quartz solid solution as the crystal phase, as developed by Nippon Electric Glass Co. (Japan), under the name of Neoceram® N-0 [22].

Solar cells and photonic devices require high transmission and efficient luminescence, respectively. TGC containing Cr-doped mullite can be used both in laser applications and solar concentrators [5].

2.1. Photonics applications

Photonics may be defined as the technology of information transfer by means of light [23]. Optical non-linearity of materials forms the basis of this ultimate technological revolution, which follows the electronics era.

2.1.1. Laser emission

A laser is a source of monochromatic radiation of high intensity, coherence and directionality, in the ultraviolet, visible or infrared optical regions. The laser mechanism is based on the radiative process of stimulated emission. A requirement of laser action is the existence of a metastable excited state with a long lifetime, as the starting level of stimulated emission. Another requirement is the existence of a larger population in this initial metastable state than in the final state, corresponding to the phenomenon of population inversion [24].

Three or four energy-level schemes are used to reach these emission processes, responsible for laser action. The energy levels involved belong to rare-earth (RE) or transition-metal ions. Of special concern for laser action are the non-radiative transitions that lead to undesirable energy dissipation. In glass, the non-radiative transitions of RE ions are accomplished by a series of different mechanisms – multiphonon relaxation, cross-relaxation and co-operative up-conversion. Multiphonon relaxation occurs by a simultaneous creation of several phonons, which suffice to equal the energy of the transition between the excited level and the next lower level; when this is larger than the highest vibrational energy of the solid matrix, several phonons may have to be created in order to bridge the energy gap. Since the probability for multiphonon decay decreases exponentially with the number of required phonons [25], it is desirable to surround the active ion by a matrix that possesses low vibrational energies. In glasses, the highest energy vibrations are stretchings of the anions against the glass forming cations, whose frequency varies with the glass composition. The highest vibrational energies in various types of glasses are listed in Table 1 [26].

Table 1. Highest vibrational energies, $h\nu$ (cm^{-1}), in inorganic glasses [26].

Glasses	$h\nu$ (cm^{-1})
Silicate	1000–1100
Germanate	800–975
Tellurite	600–850
Fluoride	500–600
Chalcogenide	200–300
$LaBr_3$	175

The presence of residual OH species in the glass host increases the non-radiative decay rates, because of coupling between the RE states and the high energy stretching vibrations of the OH groups (~3200 cm^{-1}). This contribution to non-radiative decay is very important in the case of the Er^{3+} ion, since two OH phonons are sufficient to bridge the energy gap between the $^4I_{13/2}$ and $^4I_{15/2}$ levels. Therefore, the residual OH content of the glass must be controlled to be as low as possible [24].

The other two dissipative processes – cross-relaxation and co-operative up-conversion – both involve RE ion–ion interactions, wherein the intensity of fluorescence decreases as the concentration of the active ions increases. Cross-relaxation may take place between any two closed spaced RE ions that happen to have two pairs of energy levels separated by the same amount. One of the ions, in an excited state, gives half of its energy to a ground state ion, so that both ions end up in the intermediate level. From this level, they both relax quickly to the ground state, via multiphonon relaxation. The cross-relaxation process is believed to be the dominant factor in the concentration quenching of Nd^{3+} in glass matrices [24]. The spontaneous co-operative up-conversion process may occur when two neighbouring ions are in an excited state: one of them, A, gives its energy to the other, B, thus promoting B to a higher level, while A relaxes to the ground state. From this higher energy level, the B ion relaxes rapidly, radiatively or non-radiatively. This co-operative up-conversion process is believed to be the major cause of concentration quenching in Er^{3+}-doped glasses. Er^{3+} has no intermediate states between the $^4I_{13/2}$ metastable level and the ground state, thus cross-relaxation between an excited ion and one in the ground state cannot occur [24].

RE ions of the lanthanide series have been the most extensively used active ions for laser operation, because there are a large number of fluorescing states and wavelengths to choose among the 4f electron configurations, as illustrated in Fig. 1, for some of the more commonly used RE ions. Nevertheless, one of

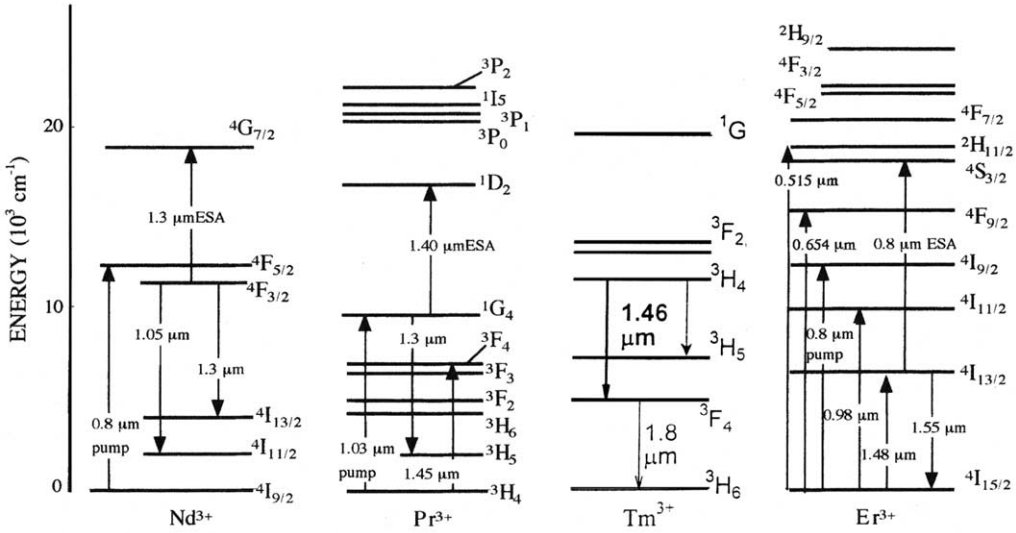

Fig. 1. Simplified electronic energy level diagrams of three different RE ions and relevant transitions for pumping and emission. (Adapted from ref. [24].)

the obstacles to the use of RE ions can be a short lifetime of the excited states and non-radiative decay paths, which depend on the local environment of the ion and on the matrix vibrational energies. Thus, the efficiency of the radiative decay in oxide glasses is generally low, compared with halide and sulphide glasses (cf. Table 1). Of the many RE ions, Er^{3+} is well known for its favourable characteristics for laser transition. Er^{3+} ions operate as a three-level system, through the $^4I_{13/2}$–$^4I_{15/2}$ transition [27–30]. They can be pumped directly into the metastable upper lasing level $^4I_{13/2}$ (1.49 μm), or into higher levels, from which non-radiative decay occurs to the metastable $^4I_{13/2}$ level. The lower lasing level, in this case, is the ground state ($^4I_{15/2}$). Absorption of lasing photons from the ground state directly to the upper lasing level may take place, causing competition with the emission of lasing photons, a phenomenon known as self-absorption, typical of three-level systems [24].

2.1.2. Frequency up-conversion

At present, there is great interest in luminescent materials for efficient frequency conversion from infrared to visible radiation, mainly because a visible source pumped by a near infrared laser is useful for high-capacity data storage optical devices. This stimulated excitation process is designated by up-conversion and is a particular type of laser action. Therefore, both the fluorescence lifetime and the stimulated emission cross-section of the RE excited level should be maximised, whereas the non-radiative decay mechanisms should be minimised. The glassy host is required to possess a minimal absorption coefficient within the wavelength region of interest, plus the capability of incorporating large RE concentrations, low vibrational energies and a high refractive index. Er^{3+} is the most commonly used RE dopant that can provide up-converted visible fluorescence, both in fluoride crystals and glasses. In conventional oxide glasses, there is no report of the up-conversion phenomenon, because of large non-radiative losses, due to high-energy vibrations, e.g. Si–O (~1100 cm^{-1}) and B–O (~1400 cm^{-1}), which couple to the Er^{3+} ions. Up-conversion pumped fluorescence expectation has therefore been placed on non-traditional oxide glass systems, with lower vibrational energies. In the stimulated up-conversion processes, excited state absorption (ESA) and energy transfer (ET) involving RE ions in the solid matrix are important mechanisms. Much work has been devoted to up-conversion lasers involving Er^{3+} ions, to produce green and red up-conversion output, respectively. The sensitisation of Er^{3+} with Yb^{3+} may also be favourable for infrared up-conversion [31–33].

2.1.3. Amplification at 1.3 and 1.5 μm

A driving force for research in RE doped fibres and integrated optics waveguides has been their use for amplifying weak signals in optical communications systems at 1.3 and 1.5 μm. This may be achieved by simply splicing a section of RE-doped fibre into the transmission one and injecting pump light through a fibre coupler. The signal generated within the RE emission band stimulates emission of radiation at the same frequency, amplifying the optical communication signal with high gain, high efficiency and low noise, which is highly advantageous for optical communications [24].

There are five main RE candidates for use as dopants in fibre or waveguide amplifiers for optical communications systems: Er^{3+}, Tm^{3+}, Nd^{3+}, Pr^{3+} and Dy^{3+}. Er^{3+} and Tm^{3+} are the choice for the 1.4–1.6-μm window centred at 1.5 μm, based on the $^4I_{13/2}$–$^4I_{15/2}$ transition of Er^{3+} and the $^3H_4$–$^3F_4$ transition of Tm^{3+}. The $^4F_{3/2}$–$^4I_{13/2}$ emission of Nd^{3+}, the $^1G_4$–$^3H_5$ transition of Pr^{3+} and the $^6F_{11/2}$ ($^6H_{9/2}$)–$^6H_{15/2}$ transition of Dy^{3+} are all potentially useful for the 1.3-μm telecommunication window.

As with the laser mechanism, the major problems concerning amplification efficiency are related to dissipative processes. In addition to all the non-radiative relaxation processes already mentioned – multiphonon relaxation, cross-relaxation and co-operative up-conversion – other dissipative processes may decrease the amplification efficiency. The phenomena of excited-state absorption (ESA) and amplified spontaneous emission (ASE) are two of the most compromising processes, which can be partially eliminated by changing the glass composition.

2.2. Glass ceramics for photonics

2.2.1. Silicate oxyfluoride glass ceramics

Glass can play many varied roles in RE laser systems, namely as the laser host medium. Fluoride glasses and crystals are highly transparent materials, from the near-UV to the middle IR, with excellent RE ion solubility and low vibrational energies, making them excellent candidates as laser host materials [34], when compared to oxide glasses such as the silicates, which have limited transparency (from ~300–3000 nm) and RE solubility. The combination of high optical transparency, large stimulated emission cross-section and low non-radiative relaxation rates enhances the probabilities of observing fluorescent emissions that are normally quenched in oxide glasses. Nevertheless, fluoride glasses have less favourable chemical, thermal and mechanical properties, compared to oxide glasses and, as a result, are difficult to prepare and to handle [34]. In fact, most oxide glasses are much more attractive from the point of view of chemical and mechanical stabilities and are easier to melt and to fabricated as rods, optical fibres, or planar waveguides than fluoride glasses.

Early in 1975, Auzel et al. [35] reported a class of partially crystalline infrared up-conversion materials which were prepared from classical glass forming oxides such as SiO_2, GeO_2 and P_2O_5, mixed with PbF_2 and a RE oxide, which showed a luminescence efficiency nearly twice as high as the LaF_3:Yb:Er phosphor. Since these materials were formed by a glass matrix and a crystal phase as large as 10 μm, they were not transparent.

More recently, in 1993, Wang and Ohwaki [36] reported for the first time a transparent and optically isotropic oxyfluoride glass-ceramic, based on a cubic fluoride crystal phase, containing Er^{3+} and Yb^{3+} ions, dispersed throughout a continuous aluminosilicate base glass. This TGC was shown to combine the optical advantages of RE-doped fluoride crystals with the ease of forming and handling of conventional oxide glasses. From the X-ray diffraction peak widths and the Scherrer formula, 20-nm nanocrystals, tentatively identified as cadmium lead fluoride, $Pb_xCd_{1-x}F_2$, were found to precipitate from the precursor aluminosilicate glasses through a suitable heat treatment. The resonant energy transfer between ytterbium and erbium was used to produce up-conversion and fluorescence in the red–green region. With an excitation wavelength of 0.97 μm, the measured up-conversion emission intensity from the glass-ceramic was 100 times that of the precursor oxyfluoride glass and 2–10 times that of a fluoroaluminosilicate glass [36], indicating excellent up-conversion efficiency and strongly suggesting the segregation of Yb^{3+} and Er^{3+} ions within $Pb_xCd_{1-x}F_2$ nanocrystals. The authors attributed this enhanced up-converted (anti-Stokes) fluorescence to a more efficient energy transfer from Yb^{3+} to the $^4F_{9/2}$ and $^4S_{3/2}$ states of Er^{3+}. These oxyfluoride glass ceramics have potential application in blue–green laser devices and also as hosts for Pr^{3+}, in amplifiers for the 1.3-μm telecommunication window. However, the crystals have a cubic lattice structure and this limits the concentration of some of the trivalent RE elements, which can be incorporated into the crystal phase. Another problem with these materials is that they require cadmium in the formulation; so this type of glass might not be desirable for a large-scale manufacturing operation.

Tick et al. [37] fabricated ytterbium-free oxyfluoride glass ceramics containing yttrium and zinc fluorides and praseodymium-doped nanocrystals of cadmium lead fluorides. The crystallite sizes were estimated from the X-ray line width of the strongest two peaks and the volume fraction of crystalline phase was estimated by integrating the area of the peaks and comparing it to the total area of the glassy halo, indicating that these glass ceramics contained 15–30% by volume of crystals, with sizes between 9–18 nm. Since these nanocrystals were believed to correspond to a Cd–Pb-rich fluoride composition, with a refractive index as large as 1.8, and the residual host glass had to be an aluminosilicate, with a refractive index as low as 1.5, the scattering Hopper model [21] indicated that the essential condition for high transparency was a structure comprised of uniformly dispersed nanoparticles, with interparticle spacing of dimensions comparable to the particle size. As long as both the

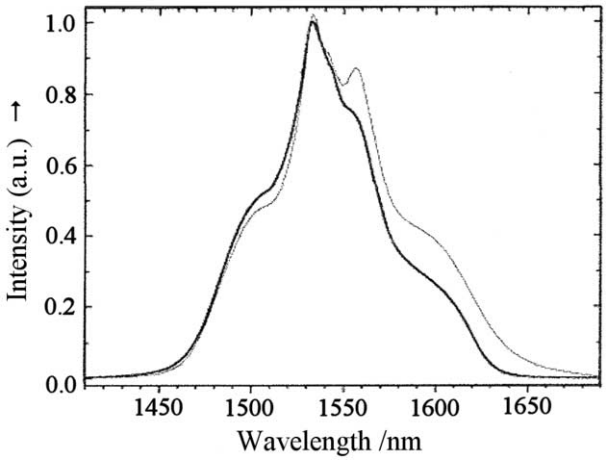

Fig. 2. Normalised photoluminescence spectra of Er^{3+} ($^4I_{13/2} \rightarrow {}^4I_{15/2}$ transition) in the precursor oxyfluoride glass (thick solid line) and in a developed glass ceramic heat treated at 440 °C for 5 h (dashed line). (Adapted from ref. [38].)

particle size and interparticle spacing remained of the order of a few tens of nanometers or less, refractive index matching was not essential in achieving high transparency, within this quasi-continuous solid approach.

Kukkonen et al. [38], based on high resolution transmission electron microscopy, have discussed the crystallisation mechanism of the above oxyfluoride glasses upon heat treatment and have proposed that the oxyfluoride phase separates to a mainly PbF_2 crystalline phase, hosting the Er^{3+} dopant and not to a more complex solid solution of CdF_2 with PbF_2, i.e., $Pb_xCd_{1-x}F_2$. The broadest and flattest emission spectrum of Er^{3+} for the $^4I_{13/2} \rightarrow {}^4I_{5/2}$ transition was recently reported for a cerammed SiO_2–Al_2O_3–CdF_2–PbF_2–ZnF_2 glass precursor composition, where 2–12-nm β-PbF_2 crystals, hosting Er^{3+} dopant ions, had developed [39], whose photoluminescence spectra are shown in Fig. 2. This glass ceramic may be important for the reduction of self-absorption and the respective noise in EDFA's. These authors reported also a new glass-ceramic type, denominated *quasi-crystal*, with a typical size of nanocrystals (or embryos) of 2–3 nm. The emission intensity of Er^{3+}-doped quasi-glass ceramic was flat across the 1530–1560 nm range, which falls in the most often employed C-band of Dense Wavelength Division Multiplexing (DWDM) systems [39].

Méndez-Ramos et al. [40] reported the optical properties of Eu^{3+} ions in oxyfluoride glass ceramics with the precursor glass composition 30 SiO_2–15 Al_2O_3–29 CdF_2–22 PbF_2–1.5 YF_3 (in mol%). The ceramming process in these oxyfluoride glasses produced a glass ceramic where EuF_3 crystals were initially produced and then acted as a nucleating agent for $Pb_xCd_{1-x}F_2$ crystal formation. A lifetime of 5.4 ms, obtained for the $^5D_0$ level of the Eu^{3+} ions in EuF_3 crystals, was close to the value of 4.5 ms, measured in the glass ceramic.

Fibres can be drawn from these TGC materials, for amplifiers operating at 1.3 μm. A Pr^{3+} fluorescence band wider than in fluorozirconate glasses has been found [41]. Tick et al. [42] measured the passive scattering losses in near single mode fibres, with TGC composition cores [37]. Using difference spectra, those authors showed that the incremental intrinsic losses in these glass-ceramic structures were in the neighbourhood of 100 dB km^{-1} [42].

It is not necessary to have all the RE ions inside the crystalline phase. For certain applications, such as gain-flattened amplifiers for DWDM systems, for example, a combination of Er^{3+} ions in the glass matrix and in the crystalline phase may be optimal. The quantum efficiencies, obtained from the ratio of the measured lifetime to the radiative lifetime calculated using the Judd–Ofelt theory [43, 44], have been given by Quimby et al. [45] and later by Méndez-Ramos et al. [46], for the two glass ceramics reported by Tick et al. [37], with values between 8–9%, as shown in Table 2.

Another family of oxyfluoride TGC, based on 15-nm crystals of LaF_3 in a sodium aluminosilicate

Table 2. Composition and properties of some glasses and corresponding transparent oxyfluoride glass ceramics (adapted from refs [20, 37]).

	Y. Wang and J. Ohwaki [36]	P.A. Tick et al. [37]	M.J. Dejneka [48]	Y. Kawamoto et al. [51]
Base glass composition (mol%)	30 SiO_2–15 $AlO_{1.5}$–24 PbF_2–20 CdF_2–10 YbF_3–1 ErF_3	30 SiO_2–15 $AlO_{1.5}$–17 PbF_2–29 CdF_2–4 YF_3–5 ZnF_2	48.5 SiO_2–25.1 $AlO_{1.5}$–13.1 LaF_3–2.5 AlF_3–10.7 Na_2O–0.1 ErF_3	50 SiO_2–50 PbF_2–x ErF_3 (x = 4 and 5)
Glass host	SiO_2–Al_2O_3	SiO_2–Al_2O_3	SiO_2–Al_2O_3–Na_2O	SiO_2
Crystal phase	$Pb_xCd_{1-x}F_2$	(Cd, Pb, Zn, Y) $F_{2.3}$	LaF_3–0.1 ErF_3	β-PbF_2:Er^{3+}
Cubic lattice parameter (nm)	0.572	0.575	—	0.582
Crystal dimension (nm)	20	9–18	15	13
Volume fraction (vol%)		20–30		
Refractive index	—	1.75	1.55	—
CTE ($\times 10^{-7}$ °C^{-1})	—	110	—	—
T_g (°C)	400	395	570	—

glass, has been proposed by Dejneka [47, 48]. LaF_3 is an ideal low-phonon host for RE cations [49], due to its ability to form extensive solid solutions with all the RE ions [50]. Emission spectroscopy showed a partition of the Eu^{3+} ions between the low-phonon-energy LaF_3 crystal and the glass host material. In fact, Eu^{3+}-doped glasses emit only red luminescence from the $^5D_0$ level, but, after a suitable heat treatment, they emit blue and green luminescence as well, indicative of a low phonon energy RE environment. Er^{3+} fluorescence and lifetime measurements in this material showed a large width and flatness for the 1530 nm emission, suggesting a good amplifier performance.

Kawamoto et al. [51] found that oxyfluoride glasses can be obtained in the SiO_2–PbF_2–ErF_3 system and heat treatment of these glasses yielded TGC in which β-PbF_2: Er^{3+} crystallites were dispersed in the glass matrix. The Scherrer equation yielded an average crystallite diameter near 13 nm. The diffraction peaks of the crystalline precipitate could be indexed in terms of the fluorite structure (space group: $Fm3m$), with a lattice constant $a = 0.582$ nm. The lattice constant of the β-PbF_2 crystal, with the fluorite structure, is $a = 0.594$ nm [52]. The slightly smaller lattice constant of the present crystalline precipitate indicated that it was a solid solution of the type β-PbF_2:Er^{3+}, in which the Pb^{2+} ions, with an ionic radius of 0.129 nm, were partially substituted by Er^{3+} ions, with an ionic radius of 0.100 nm. These glass ceramics had highly efficient up-conversion luminescence, under 800 nm laser excitation.

The composition and properties of the oxyfluoride glass ceramics are summarised in Table 2. Clearly, three main types of optically transparent, silica-based glass ceramics have been achieved: (*i*) those prepared by Wang and Ohwaki [36] and Tick et al. [37], based upon the formation of a (Pb, Cd)F_2 cubic phase, incorporating Er^{3+}/Yb^{3+} or Pr^{3+}, in an aluminosilicate base glass; (*ii*) a second type, formed by LaF_3 crystals in a sodium aluminosilicate base glass, reported by Dejneka [47]; finally, (*iii*) a third type, where β-PbF_2:Er^{3+} crystallites are dispersed in a silica glass matrix, as reported by Kawamoto et al. [51].

All the above transparent silica-based glass ceramics are not only very stable, but also all melting and processing can be done in platinum crucibles in air, at temperatures between 1000 and 1200 °C. Afterwards, the precursor glass is thermally treated at a temperature that is usually that of a crystallisation peak that lies just above T_g. The optimum ceramming temperature normally lies between the onset and the peak maximum of the crystallisation exotherm.

It has been found that the presence of the RE elements is needed in order to obtain a low temperature

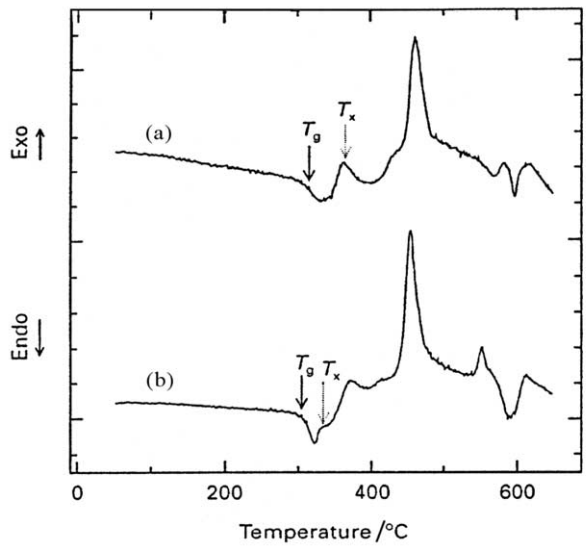

Fig. 3. DTA curves of the glass compositions 50 SiO_2–50 PbF_2–x ErF_3, (**a**) $x = 3$ and (**b**) $x = 5$ (in mol%). (Adapted from ref. [51].)

crystallisation peak in these silicate-based systems, as illustrated in Fig. 3. The corresponding XRD patterns for the composition with 5% Er are shown in Fig. 4. Braglia et al. [41] pointed out that primary crystallisation is of paramount relevance in these oxyfluoride systems, since the photoluminescence intensity increased as the transformation to the nanocrystalline phase progressed. This finding was an indication that the surroundings of the RE ions were changed by the formation of crystallites, because of the ion migration either into these crystals, or toward the nanocrystal/glass boundaries.

The high-temperature properties of all these oxyfluoride glass ceramics, in which the optically active

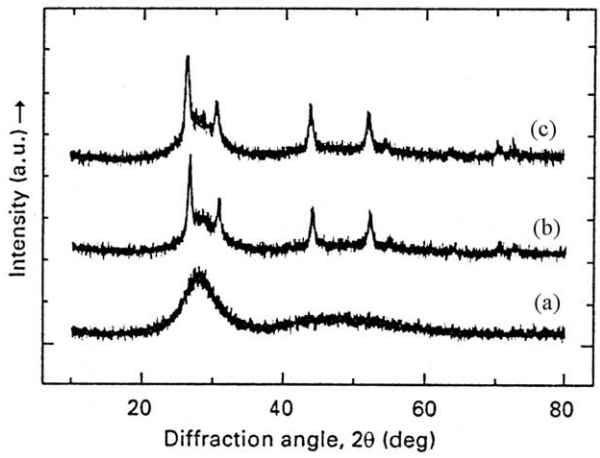

Fig. 4. XRD patterns of 50 SiO_2–50 PbF_2–5 ErF_3 (mol%) glass, heat treated at the first crystallisation temperature, T_x, for (**a**) 0 h, (**b**) 0.5 h and (**c**) 6 h. (Adapted from ref. [51].)

RE ions partition into a fluoride crystal phase, are more like those of an oxide than a fluoride glass. Oxyfluoride glass ceramics offer an economic alternative, with substantial performance improvements, over purely fluoride glasses. They combine the attributes of the fluoride crystal phase with those of a conventional silica-based glass matrix. A patent has already been registered with some of these glass compositions [53].

2.2.2. Germanate-oxyfluoride glass ceramics

Lead germanate oxyfluoride TGC were obtained in 1995 by Hirao et al. [54], in the GeO_2–PbO–PbF_2–TmF_3 system, containing ~16 nm β-PbF_2:Tm^{3+} crystals. Bueno et al. [55] and Mortier and Auzel [56] studied the GeO_2–PbO–PbF_2–CdF_2 and GeO_2–PbO–PbF_2 Er^{3+}-doped systems, respectively. Both groups obtained cubic β-PbF_2:Er^{3+}nanocrystallites ~5–10 nm and ~8–20 nm in size, respectively, in TGC materials. Mortier et al. [56] measured the lifetime of the $^4I_{11/2} \rightarrow {}^4I_{13/2}$ transition of Er^{3+} around 2.7 μm, in germanate glasses of composition 50 GeO_2–40 PbO–10 PbF_2 (mol%) doped with 1–4 mol% ErF_3, before and after heat treatment, and found an increase from 360 μs to 3 ms with the nanocrystallisation, for 3 mol% Er^{3+}, which was still less than the 7 ms of crystalline PbF_2 doped with 1 mol% ErF_3 [56, 57], suggesting that only some of the Er^{3+} ions were incorporated into β-PbF_2 crystals.

Germanate oxyfluoride TGC were also obtained for higher concentrations of PbF_2 and infrared up-conversion to the visible and near UV regions was observed in Yb-doped PbF_2–GeO_2–Al_2O_3–Tm_2O_3 glasses and glass ceramics [58], as shown in Fig. 5. Improved fluorescence was also obtained for Tm^{3+} precipitated in PbF_2 nanocrystals, upon cerammisation of germano-silicate oxyfluoride glass [59]. When compared with the glasses, the lifetime of the TGC compositions increased from ~400 to ~500 μs at 1.4 μm and remained unchanged at ~5.0 ms at 1.8 μm.

2.2.3. Tellurite oxyhalide glass ceramics

The search for other glass precursors for TGC has been motivated by the limited RE solubility and small non-linear behaviour of silica-based compositions, as well as the low chemical durability of purely fluoride compositions. Tellurite glasses have the lowest vibrational energies (~ 700 cm^{-1}) among oxide glasses (cf. Table 1), large refractive indices ($n \sim 2$), large RE solubility and low melting points [60], thus suggesting their high potential as new optical functional materials, for optical amplifiers, frequency up-converters and lasers.

Although RE doped TeO_2-based glasses have been extensively studied by several authors [61], there is very little information on TeO_2-based TGC. Developed by Shioya et al. [62], the first TeO_2-based TGC consisted of an unknown cubic crystalline phase with an average diameter of ~20–40 nm, crystallised from a 70 TeO_2–15 Nb_2O_5–15 K_2O glass composition (mol%). This glass ceramic presented better optical and dielectric properties than those of the parent glass and second-harmonic generation (SHG) was achieved [62, 63]. Oishi et al. [64] doped this composition (modified with MgO), with 1.2 mol% Er^{3+} and Eu^{3+} and optically TGC could be obtained, presenting higher up-conversion fluorescence intensity around 550 nm than the corresponding TeO_2-based glass precursors. It was also shown [65] that cerammisation of these glasses raised their Vickers hardness values, improving their mechanical properties. Hirano et al. [66] introduced several RE ions in the same system and obtained up-conversion fluorescence intensities about 20 times higher than in the corresponding 70 TeO_2–15 Nb_2O_5–15 K_2O glass composition, with 1 mol% Er_2O_3.

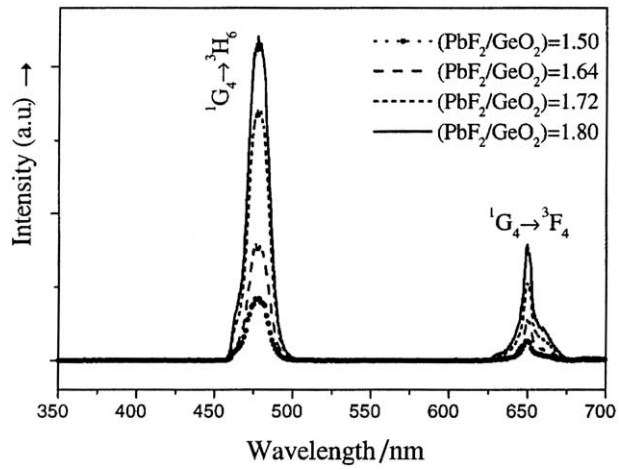

Fig. 5. Up-conversion emission spectra of Tm^{3+}/Yb^{3+}-co-doped PbF_2–GeO_2–Al_2O_3 glass ceramics, containing 3 mol% Al_2O_3, as a function of the PbF_2/GeO_2 ratio. (Adapted from ref. [58].)

Recently, tellurium oxyfluoride TGC have also been obtained [67] with the composition 80 TeO_2–10 PbF_2–10 CdF_2 (mol%), whose crystalline phase was identified to be $PbTe_3O_7$, by XRD and EXAFS, but no information was given concerning their luminescence properties. Erbium-doped tellurium oxyhalide TGC have also recently been obtained in the TeO_2–ZnO–$ZnCl_2$ system, for the 60 TeO_2–20 ZnO–20 $ZnCl_2$ and 40 TeO_2–20 ZnO–40 $ZnCl_2$ (mol%) compositions doped with 1–10 mol% $ErCl_3$ [68]. The precursor tellurite glasses, modified by zinc or lead oxide plus the corresponding halides, have been investigated [69] and the corresponding glass-forming regions were determined. Compositions in the TeO_2–ZnO–ZnX_2 and TeO_2–PbO–PbX_2 glass systems, in particular with X = Cl, yielded stable glasses of

good optical quality. TeO_2–ZnO–$ZnCl_2$ glasses with 20 mol% ZnO were selected as hosts for $ErCl_3$, up to 10 mol%. The 1.5-μm photoluminescence spectra and metastable level lifetimes of Er^{3+} in these glasses, especially with ~ 3–5 mol% $ErCl_3$, suggest that they may be suitable for optical amplifier applications [69]. A measured lifetime of ~ 7 ms, was obtained for the $^4I_{13/2} \rightarrow {}^4I_{15/2}$ transition of Er^{3+}, in these tellurite glass ceramic [68].

2.2.4. Other glass ceramic compositions

Purely fluoride TGC have been prepared by Jewell et al. [70] in a ZrF_4-doped CLAP (CdF_2–LiF–AlF_3–PbF_2) glass. According to the authors, more than 80% transmission in the visible was achieved, even for 95% crystallisation. Mortier et al. [71] also prepared TGC in a fluoride system (ZrF_4–LaF_3–ErF_3–GaF_3–AlF_3), by liquid–liquid phase separation, resulting in spinodal decomposition. Good transparency was obtained for a high crystallisation level (90%), due to a good refractive index matching between the glass and crystal phases.

Fluorescence was observed in europium-doped fluorobromozirconate TGC [72], where Eu^{2+} ions were believed to precipitate in $BaBr_2$ crystals.

Recently, lithium–borate-oxide-based TGC have been synthesised in the $Li_2B_4O_7$–Bi_2WO_6 [73] and $Li_2B_4O_7$–SrO–Bi_2O_3–Nb_2O_5 systems [74], comprising spherical ferroelectric nanocrystalline phases: Bi_2WO_6, with ~2–33 nm and $SrBi_2Nb_2O_9$, with ~20 nm, respectively, embedded in a $Li_2B_4O_7$ glass matrix. These glass ceramics have increased dielectric constants and low dielectric losses, when compared with the parent glasses, as well as high second-harmonic generation efficiencies.

TGC can also be efficient hosts for transition metal ions, as demonstrated by Beall [75] for Cr^{4+}-doped forsterite (Mg_2SiO_4) and Pinckney et al. [76], with Ni^{2+}-doped gallate spinel. Beall isolated a forsterite-rich glass composition via nanoscale phase separation in the SiO_2–Al_2O_3–MgO–K_2O system. When doped with chromium oxide, both Cr^{4+} luminescence and absorption became similar to those of single crystals. However, transparency was only achieved with the addition of TiO_2 as a nucleating agent.

3. Conclusions

TGC have a number of useful properties, especially for photonics applications. Here, the precipitation of a fluoride or other halide crystalline phase with low maximum vibrational energy, containing a RE ion such as Er^{3+}, within an oxide or oxyhalide glass matrix of high stability, achieves improved luminescence properties for the RE ion, without sacrificing good glass-forming ability, glass stability and ease of glass fabrication. Therefore, TGC is a very promising new type of photonic material.

References

[1] S.D. Stookey, Ind. Eng. Chem. 45 (1953) 115.

[2] S.D. Stookey, Photosensitively Opacifiable Glass, US Patent No. 2 684 911, 1954.

[3] S.D. Stookey, Ind. Eng. Chem. 51 (1959) 805.

[4] S.D. Stookey, Ceramic Body and Method of Making It, US Patent No. 2 971 853, 1961.

[5] W. Höland, G. Beall, Glass Ceramic Technology, The American Ceramic Society, 2002.

[6] M. Réaumur, Mém. Acad. R. Sci. Paris (1739) 370.

[7] Pyroflam®, Registered Newell SA Trademark.

[8] Visions®, Registered Corning Glass Works Trademark.

[9] Z. Strnad, Glass Ceramic Materials, Elsevier, Amsterdam, The Netherlands, 1986.

[10] (a) Fotoform®, Fotoceram®, Registered Corning Glass Works Trademarks; (b) G.H. Beall, Annu. Rev. Mater. Sci. 22 (1992) 91.

[11] Foturan®, Registered Schott Glaswerke and mtg Mikroglas Technik AG, Mainz, Germany Trademark.

[12] Bioglass®, Registered US Trademark, University of Florida, Gainesville, FL, USA, 32611.

[13] R. Li, A.E. Clark, L.L. Hench, J. Appl. Biomater. 2 (1991) 231.

[14] H. Brömer, E. Pfeil, H.H. Käs, German Patent No. 2 326 100, 1973.

[15] T. Kokubo, Glastech. Ber. 67C (1994) 105.

[16] D.G. Grossmann, Am. Machinist (May 1978) 139.

[17] K.A. Malament, D.G. Grossman, J. Prosthetic Dent. 57 (1987) 674.

[18] W. Vogel, W. Höland, Angew. Chem. Int. Ed. Engl. 26 (1987) 527.

[19] Schott Glaswerke Mainz, Brochure No. 10041, 1991.

[20] G.H. Beall, L.R. Pinckney, J. Am. Ceram. Soc. 82 (1999) 5.

[21] R.W. Hopper, J. Non-Cryst. Solids 70 (1985) 111.

[22] Neoceram®, Registered Nippon Electric Glass Trademark.

[23] P.A. Tick, Extended Abstracts of the International Symposium on Non-Oxide Glasses, Sheffield, UK, 1998, p. 14.

[24] M. Yamane, Y. Asahara, Glasses for Photonics, Cambridge University Press, Cambridge, UK, 2002.

[25] T. Miyakawa, D.L. Dexter, Phys. Rev. B 1 (1970) 2961.

[26] R. Reisfeld, C.K. Jorgensen, Excited State Phenomena in Vitreous Materials, in: K.A. Gschneidner Jr, L. Eyring (Eds.), Handbook on the Physics and Chemistry of Rare Earths, Vol. 9, North Holland, Amsterdam, 1987, p. 1.

[27] M.J. Weber, Non-Metallic Compound II, in: K.A. Gschneidner Jr, L.R. Eyring (Eds.), Handbook on the Physics and Chemistry of Rare Earths, Vol. 4, Chap. 35, North-Holland Physics Publishing, Amsterdam, 1979, p. 275.

[28] D.W. Hall, M.J. Weber, in: M.J. Weber (Ed.), CRC Handbook of Laser Science and Technology, Supplement 1: Lasers, CRC Press, Boca Raton, 1991, p. 137.

[29] M.J. Weber, J. Non-Crystalline Solids 123 (1990) 208.

[30] J.A. Caird, S.A. Payne, M.J. Weber (Eds.), CRC Handbook of Laser Science and Technology, Supplement 1, Lasers, CRC Press. Boca Raton, 1991, p. 3.

[31] F. Auzel, J. Lumin. 45 (1990) 341.

[32] Y. Mita, K. Hirama, N. Ando, H. Yamamoto, S. Shionoya, J. Appl. Phys. 74 (1993) 4703.

[33] Y. Mita, J. Appl. Phys. 43 (1972) 1772.

[34] R.M. Almeida, Fluoride Glasses, in: K.A. Gschneidner Jr, L. Eyring (Eds.), Handbook on the Physics and Chemistry of Rare Earths, Vol. 15, Elsevier Science Publishers, 1991, p. 287.

[35] F. Auzel, D. Pecile, D. Morin, J. Electrochem. Soc. 122 (1975) 101.

[36] Y. Wang, J. Ohwaki, Appl. Phys. Lett. 63 (1993) 3268.

[37] P.A. Tick, N.F. Borrelli, L.K. Cornelius, M.A. Newhouse, J. Appl. Phys. 78 (1995) 93.

[38] L.L. Kukkonen, I.M. Reaney, D. Furniss, M.G. Pellat, A.B. Seddon, J. Non-Cryst. Solids 290 (2001) 25.

[39] V.K. Tikhomirov, D. Furniss, A.B. Seddon, M. Ferrari, R. Rolli, J. Mater. Sci. Lett. 21 (2002) 293.

[40] J. Mendéz-Ramos, V. Lavín, I.R. Martín, U.R. Rodríguez-Mendoza, V.D. Rodríguez, D. Lozano-Gorrín, P. Núñez, J. Appl. Phys. 89 (2001) 5307.

[41] M. Braglia, C. Bruschi, G. Dai, J. Kraus, S. Mosso, M. Baricco, L. Battezzati, F. Rossi, J. Non-Cryst. Solids 256–257 (1999) 170.

[42] P.A. Tick, N.F. Borrelli, I.M. Reaney, Opt. Mater. 15 (2000) 81.

[43] B.R. Judd, Phys. Rev. 127 (1962) 750.

[44] G.S. Ofelt, J. Chem. Phys. 37 (1962) 511.

[45] R.S. Quimby, P.A. Tick, N.F. Borrelli, L.K. Cornelius, J. Appl. Phys. 83 (1998) 1649.

[46] J. Méndez-Ramos, V. Lavín, I.R. Martín, U.R. Rodríguez-Mendoza, J. González-Almeida, V.D. Rodríguez, D. Lozano-Gorrín, P. Núnez, J. Alloys Compds 323–324 (2001) 753.

[47] M.J Dejneka, Proc. SPIE 3280 (1998) 132.

[48] M.J. Dejneka, J. Non-Cryst. Solids 239 (1998) 149.

[49] M.J. Weber, J. Chem. Phys. 48 (1968) 4774.

[50] O.V. Kudryavteseva, L.S. Garashina, K.K. Rivkina, B.P. Sobolev, Sov. Phys. Crystallogr. 18 (1974) 531.

[51] Y. Kawamoto, R. Kanno, J. Qiu, J. Mater. Sci. 33 (1998) 63.

[52] JCPDS International Centre for Diffraction Data Card No. 6-0251.

[53] P. Tick, United States Patent, No. US 6 281 151 B1, 28 August 2001.

[54] K. Hirao, K. Tanaka, M. Makita, N. Soga, J. Appl. Phys. 78 (1995) 3445.

[55] L.A. Bueno, P. Melnikov, Y. Messaddeq, S.L.J. Ribeiro, J. Non-Cryst. Solids 247 (1999) 87.

[56] M. Mortier, F. Auzel, J. Non-Cryst. Solids 256–257 (1999) 361.

[57] M. Mortier, P. Goldner, C. Château, M. Genotelle, J. Alloys Compds 323–324 (2001) 245.

[58] F.C. Guinhos, P.C. Nóbrega, P.A. Santa-Cruz, J. Alloys Compds 323–324 (2001) 358.

[59] H. Hayashi, S. Tanabe, T. Hanada, J. Appl. Phys. 89 (2001) 1041.

[60] J.S. Wang, E.M. Vogel, E. Snitzer, Opt. Mater. 3 (1994) 187.

[61] R.A.H. El-Mallawany, Tellurite Glasses Handbook – Physical Properties and Data, CRC Press, Boca Raton, 2001.

[62] K. Shioya, T. Komatsu, H.G. Kim, R. Sato, K. Matusita, J. Non-Cryst. Solids 189 (1995) 16.

[63] H.G. Kim, T. Komatsu, K. Shioya, K. Matusita, K. Tanaka, K. Hirao, J. Non-Cryst. Solids 208 (1996) 303.

[64] H. Oishi, Y. Benino, T. Komatsu, Phys. Chem. Glasses 40 (1999) 212.

[65] T. Watanabe, Y. Benino, K. Ishizaki, T. Komatsu, J. Ceram. Soc. Jpn 107 (1999) 1140.

[66] K. Hirano, Y. Benino, T. Komatsu, J. Phys. Chem. Solids 62 (2001) 2075.

[67] M.A.P. Silva, Y. Messaddeq, V. Briois, M. Poulain, F. Villain, S.J.L. Ribeiro, J. Phys. Chem. Solids 63 (2002) 605.

[68] Luís M. Fortes, Luís F. Santos, M. Clara Gonçalves, Rui M. Almeida, unpublished work.

[69] L.M. Fortes, L.F. Santos, M. Clara Gonçalves, Rui M. Almeida (submitted for publication).

[70] J.M. Jewell, E. Joseph Friebele, Ishwar D. Aggarwal, J. Non-Cryst. Solids 188 (1995) 285.

[71] M. Mortier, A. Monteville, G. Patriarche, G. Mazé, F. Auzel, Opt. Mater. 16 (2001) 255.

[72] A. Edgar, S. Schweizer, S. Assmann, J.M. Spaeth, P.J. Newman, D.R. MacFarlane, J. Non-Cryst. Solids 284 (2001) 237.

[73] G.S. Murugan, K.B.R. Varma, J. Non-Cryst. Solids 279 (2001) 1.

[74] N. Syam Prasad, K.B.R. Varma, Mater. Sci. Eng. B90 (2002) 246.

[75] G.H. Beall, Proc. Int. Congr. Glass, Vol. 2, Edinburgh, Scotland, 2001, p. 170.

[76] L.R. Pinckney, B.N. Samson, G.H. Beall, J. Wang, Proc. 104th Annual Meeting & Exhibition, The American Ceramic Society, St. Louis, Missouri, USA, 2002, p. 120.